

~~N73-32795422~~

NASA CR-132314

OPTIMIZATION OF A CORRUGATED STIFFENED COMPOSITE

PANEL UNDER UNIAXIAL COMPRESSION

by B. L. Agarwal and L. H. Sobel

**CASE FILE  
COPY**

Prepared under Grant No. NGR 36-004-065  
University of Cincinnati  
Cincinnati, OH 45221

for

NATIONAL AERONAUTICS AND SPACE ADMINISTRATION

TABLE OF CONTENTS

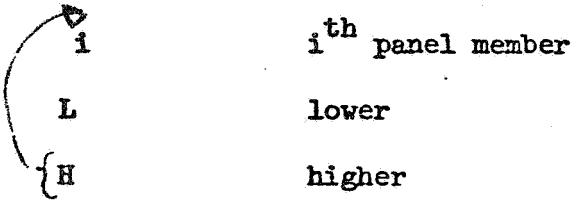
Chapter	Page
ACKNOWLEDGEMENTS . . . . .	i
NOTATIONS . . . . .	iv
TABLES . . . . .	vi
ILLUSTRATIONS . . . . .	vii
I INTRODUCTION . . . . .	I
II GENERAL APPROACH OF STRUCTURAL OPTIMIZATION. . . . .	4
2.1 Concept of optimization . . . . .	4
2.2 Optimization approaches . . . . .	4
2.2.1 Adaptive creep search. . . . .	9
2.2.2 Pattern search . . . . .	10
2.3 General structural optimization cycle . . . . .	11
III ANALYSIS . . . . .	13
3.1 Formulation of the problem. . . . .	13
3.1.1 Basic assumptions. . . . .	13
3.1.2 Performance function . . . . .	14
3.1.3 Design variables . . . . .	14
3.1.4 Constraints. . . . .	14
3.2 Stress analysis . . . . .	16
3.2.1 Load in each panel member. . . . .	16
3.2.2 Local buckling . . . . .	17
3.2.3 Euler buckling . . . . .	18

	3.3 Discussion of minimization procedure . . . . .	21
IV	NUMERICAL RESULTS . . . . .	23
V	CONCLUDING REMARKS. . . . .	28
	References. . . . .	29
	Appendix-A Optimization Technique . . . . .	31
	Appendix-B BUCLASP-2 assumptions and Model. . . . .	40

## NOTATION

$A$	cross sectional area of one pitch of the panel
$A_i$	area of the panel member
$b$	pitch of stiffner spacing
$b_i$	width of the panel member
$D_{ij}$	bending stiffness coefficients
$E_i$	Young's Modulus of the panel member
$f_i$	percentage of $\pm 45^\circ$ layers in the panel member
$L$	length of the panel
$N_{x_a}$	applied load per unit width of the panel
$N_{x \text{ Euler}}$	Euler buckling load per unit width of the panel
$P_{ai}$	applied load to the panel member
$P_{li}$	local buckling load of the panel member
$P$	total load acting on the panel per unit pitch
$t_i$	thickness of the panel member
$\bar{y}$	distance of center of effective gravity of AE distribution from the reference axis
$y_i$	distance of center of gravity of the panel member from the reference axis
$\epsilon$	strain in the panel
$\epsilon_y$	yield strain of the material
$\bar{\rho}$	weight per unit area
$\phi$	performance function
$\sigma_{ai}$	applied stress to the panel member
$\sigma_l$	local buckling stress

Subscript



$i^{\text{th}}$  panel member

lower

higher

Superscript

\* modified dimensions

o degree

TABLES

Table		Page
1	Material Properties . . . . .	58
2	Optimized design variables for graphite/epoxy panel (L = 30") . . . . .	59
3	Optimized design variables for graphite/epoxy panel (L = 40") . . . . .	60
4	Optimized design variables for graphite/epoxy panel (L = 50") . . . . .	61
5	Optimized design variables for graphite/epoxy panel (L = 30") . . . . .	62
6	Optimized design variables for graphite/epoxy panel (L = 40") . . . . .	63
7	Optimized design variables for graphite/epoxy panel (L = 50") . . . . .	64
8	Optimized design variables for all aluminum panel (L = 30") . . . . .	65

ILLUSTRATIONS

Figure		Page
1	Adaptive search combined with pattern search . . . . .	42
2	Optimization cycle . . . . .	43
3	Panel to be optimized. . . . .	44
4	Representative cross-section of the panel. . . . .	45
5	Equivalent width . . . . .	46
6	Weight strength plot for all composite and all aluminum panel . . . . .	47
7	Optimized sections (Full scale). . . . .	48
8	Buckling modes . . . . .	49

INTRODUCTION

Optimization of structural members has been a very intriguing topic of investigation in the past two decades (References 1-2). Development of new structural materials, such as composites, and a great need for light weight structures has made it even more important to find optimum designs using composite materials.

There are several different levels of abstraction at which the basic structural design problem can be approached. The most common one is to consider the optimum design of structural elements such as columns and plates and composite structures such as box beams and panels for prescribed loads and prescribed overall (loading) dimensions. Thus for individual elements, the optimum design analyses result in the specification of the cross sectional dimensions for a given loading index. In certain applications, it is meaningful to relax one of the loading dimensions of a composite structure to find a design of absolute minimum weight. In this case Becker has obtained results for the optimum structural chord for a box beam (Reference 3) and an optimum diameter for a cylinder in bending (Reference 4) by essentially adjusting the value of the loading index.

The concept of loading indices and efficiency factors have been proved very useful for the conventional isotropic materials. The development of these concepts is attributed to Zahorski (Reference 5).

They have been used very effectively by Farrar, Shanley, Gerard and others (References 6, 7, 8). The loading index concept is applied in a minimum weight or efficiency analysis by expressing the quantity to be minimized (weight) or maximized (stress) in terms of the prescribed dimensions and loads. In doing so, the general approach used by many investigators is to reduce the number of unknown dimensions to two or three by making suitable guess so as to the ratio of various dimensions in order to get a closed form solution.

In the present study a relatively new approach of structural optimization has been used to optimize the weight of a simply supported, corrugated hat stiffened composite panel under uniaxial compression. This approach consists of the employment of nonlinear mathematical programming techniques to reach an optimum solution. This approach is in contrast to the one for which a closed form is attempted, since for the later no simplifying assumptions are required in general with regard to the cross-sectional dimensions. However in the present work some simplifying assumptions in the stress analysis are made to effect faster convergence to an optimum solution. With these simplifying assumptions the number of unknown design parameters is reduced to twelve for the purpose of optimization. Since the number of unknown parameters in the present problem is twelve as compared to two or three in the loading index approach, twelve simultaneous equations are needed to get values of all the unknown parameters. Hence, in the loading index approach, either further simplifying assumptions have to be made for the dimensions of the cross section or a more involved stress analysis describing

the behavior of failure is required. For example, in buckling problems additional modes of failure have to be considered.

In the present analysis, a computer code (Reference 9) called AESOP (Automated Engineering and Scientific Optimization Program) is used for the optimization studies.

AESOP consists of several optimum search algorithms. Depending upon the behavior of the performance function (weight), one or a combination of search algorithms can be used to find the parameters (design variables) which will minimize the performance function. AESOP is used to optimize the design parameters of the panel. Then, as a check on the effect of the simplifying assumption, the critical load for the optimized panel is obtained from BUCLASP-2 (Reference 10) and compared with the specified panel loads. Good correlation was obtained.

Unfortunately, no optimization results are available for all composite panels, for the purpose of comparison. The results for aluminum panels are available (Reference 2). A comparison of the present results was made with the available results and good correlation was found.

## II

### GENERAL APPROACH OF STRUCTURAL OPTIMIZATION

Portions of this chapter closely follow the material contained in Reference (9).

#### 2.1 Concept of optimization

In general, any optimization problem can be thought of as minimization or maximization of a performance function. For example, in structural problems, weight and stress are the performance functions. Similarly in rocket design, the range of the rocket may be taken to be a performance function. In all such optimization problems the ultimate aim is to find the value of design parameters which will optimize the performance function.

#### 2.2 Optimization approaches

There have been several different approaches used by many investigators to reach to an optimum solution. One of the most powerful techniques used until recent years for the optimization of conventional structural members is the loading index approach (Reference 2). In this approach, the loading index is expressed in terms of weight or stress and the dimensions of the structural member. In general this can be written as

$$\text{loading index} = \text{efficiency factor} \times (\text{weight index})^n \quad (1)$$

In this equation the efficiency factor is a function of geometric properties of the structure under consideration. These may be treated as independent variables in minimization of the weight. The weight index is designated as the nondimensional weight function. Minimization of weight is achieved by maximization of the efficiency factor. In equation (1)  $n$  is an exponent, whose value depends on the structure under consideration.

The basic assumption used in arriving at equation (1) for a given structural element of buckling problem is that, for optimum design, at least two lowest modes of instability are simultaneously critical under the applied loading (References 7, 11). It should be noted that in this approach the number of unknown parameters is reduced to two or three in order to get a closed form solution. The reason for doing so is obvious. For more unknown parameters, the problem becomes more complex and it becomes impossible to get closed form solutions because more modes of failure have to be considered in order to get additional equations to determine the unknown parameters.

In the present problem the loading index approach can not be used effectively because the number of unknown parameters is large. A more recent approach of structural optimization is to use nonlinear mathematical programming techniques. In this approach we are concerned with the maximization or minimization of a pay-off or performance function  $\phi$  of the form

$$\phi = \phi(\alpha_i) \quad , \quad i = 1, 2, \dots, n \quad (2)$$

subject to the array of constraints

$$C_j = C_j(\alpha_i) \quad , \quad j = 1, 2, \dots, p \quad (3)$$

The  $\alpha_i$  are the independent design variables whose values are to be determined so as to maximize or minimize the performance function  $\phi(\alpha_i)$ , subject to the constraints of equation (3). The  $\alpha_i$  may be thought upon as the components of a control vector,  $\bar{\alpha}$ , in the space  $R^N$  of dimension  $N$ . Since maximization of a function is equivalent to minimization with a change of sign, it will be sufficient to discuss the case in which performance function is to be minimized.

Multivariable optimization problems involving inequality regional constraints relating the design variables may also be encountered as follows

$$\alpha_i^L \leq \alpha_i \leq \alpha_i^H \quad (4)$$

The inequality constraints define a region of the control space within which the solution must lie. For example, in structural buckling problems, if the design variables are taken to be cross-sectional dimensions, then these dimensions neither can be less than or equal to zero nor become infinitely large. So the above limits bound the region in which these variables must lie.

Inequality constraints on the functions of independent variables similarly restrict the region in which the optimal solution is to be

obtained. In this case

$$F_K^L(\alpha_i) \leq F_K(\alpha_i) \leq F_K^H(\alpha_i) \quad (5)$$

For example, in structural buckling problem, various modes of buckling modes will constitute constraints, such that the structure is capable of carrying the design load. These constraints will be function of independent design variables.

Inequality constraints can be used to restrict the search region directly, or, alternatively, they may be transformed into equality constraints. Several transformations may be used for this purpose. For example, let an equality constraint,  $C_K$ , be defined by the transformation

$$C_K = \begin{cases} (F_K^L - F_K)^2 & ; F_K < F_K^L \\ 0 & , F_K^L \leq F_K \leq F_K^H \\ (F_K^H - F_K)^2 & , F_K^H < F_K \end{cases} \quad (6)$$

constraint  $C_K$  to zero will result in the constraint of equation (5) being satisfied.

Problems involving equality constraints can be treated as unconstrained problem by replacing the actual performance function,  $\phi(\alpha_i)$ , by a penalized performance function,  $\phi^*$ , where

$$\phi^* = \phi + \sum_{j=1}^P U_j C_j \quad (7)$$

It can be shown that, provided the positive weighting multipliers  $U_j$  are sufficiently large in magnitude, minimization of the performance function subject to the constraints of equation (3) is equivalent to minimization of the unconstrained penalized performance function defined by equation (7). This approach permits search techniques for finding unconstrained minima to be applied in the solution of constrained minima problem at the cost of some increased complexity in the behavior of the performance function. The weighting multipliers  $U_j$  are determined adaptively on the basis of response surface behavior.

Alternatives to this approach are available, notably Bryson's approach to the steepest-descent search (Reference 12). This method has been exploited in connection with the numerical solution of variational problems encountered in the optimization of aerospace vehicle flight paths (Reference 13). However the use of such techniques implies smoothness of the response surface. This smoothness can not be assumed in the problem of structural optimization in general; hence, the less restrictive penalty function approach of equation (7) is used. A detailed discussion of solution techniques is presented in appendix A, however, some of the search algorithms will be discussed below.

### 2.2.1 Adaptive creep search

This search is a form of small scale sectioning; however instead of locating the position of the one-dimensional extremal on each section parallel to a coordinate axis, the coordinate is merely perturbed by small amount,  $\Delta\alpha_r$ , in the descending direction.

The search commences with a small perturbation in one of the independent variables,  $\alpha_r$ ; a positive perturbation is first made; if this fails to produce a performance improvement, then a negative perturbation is tried. If neither of the perturbations produces an improved performance value, the variable retains its original value, and  $\Delta\alpha_r$  is halved. If a favorable perturbation is found, the variable  $\alpha_r$  is set to this value, and  $\Delta\alpha_r$  is doubled. The process is repeated for each independent variable in turn, the order in which the variables are perturbed being chosen randomly. At this point an adaptive search cycle is complete, and the cycle is then repeated. A two-dimensional illustration of this search is presented in figure (1). In the particular problem illustrated, the method converges rapidly reaching the neighborhood of the extremal within six evaluations.

The search algorithm can be written in the form

$$\Delta\alpha_r = 2.0 \frac{(S_r - T_r)}{S_r}, \text{ (DP)} \quad (8)$$

where  $S_r$  is the number of cycles in which the search has successfully perturbed the  $r^{\text{th}}$  independent variable, and  $T_r$  is the number of cycles in which the perturbation of the  $r^{\text{th}}$  variable has proved

unsuccessful. Here, the scalar quantity (DP) merely defines an initial perturbation for each independent variable. Once started the search proceeds inevitably to its conclusion, the perturbation in each independent variable being adaptively determined according to equation (8) on the basis of the performance function response contour behavior encountered during the particular problem solution. This search can be quite efficient when used in combination with the pattern search acceleration procedure.

### 2.2.2 Pattern search

In the present work, pattern search refers to a search which exploits a gross direction revealed by one of the other searches. The search algorithm is

$$\Delta\alpha_i = (\alpha_i^2 - \alpha_i^1) \cdot (DP), i = 1, 2, \dots, N \quad (9)$$

where  $\alpha_i^2$  and  $\alpha_i^1$  are the components of the control vector before and after the use of a preceding search technique. This is illustrated in figure (1) following an adaptive search. The combination of an adaptive search and a pattern search in the problem illustrated leads directly to the neighborhood of the extremal. Repeated adaptive search on the other hand, would be a very slowly converging process due to the orientation of the contours with respect to the axes of the independent variables. It may be noted that a simple rotation of the independent variable axes by  $45^\circ$  results in adaptive creep alone becoming a rapidly converging process in this example. The present

discussion of optimization concept is rather superficial. Detailed treatments may be found in (References 9, 22).

### 2.3 General structural optimization cycle

Figure (2) shows a typical optimization cycle. First of all the geometry (e.g. flat panel with corrugated hat stiffeners) of the structure, the loads, and the material are specified. An attempt is then made to find the values of design variables, which will minimize the weight of the structure. Figure (2) shows some of the design variables for a composite panel subjected to compressive loads. These design variables are

1. Cross-sectional dimensions: In the optimization problem one has to find the dimensions of the cross-section which will minimize the weight of the panel.
2. Filament orientation: This means, the orientation of filaments with respect to a reference axis.
3. Percentage of different orientations: This simply means the percentage of differently oriented laminates required in a Lamina . For example, if only two kinds of laminate orientations are used, say  $0^\circ$  and  $90^\circ$  one has to know that, how much of each is needed in a structural member to obtain the least weight design.
4. Laminating sequence: This means the sequence in which differently oriented laminates are arranged to make a structural member.

There could be more design variables depending upon the need of the problem under investigation. In order to find the value of these design

variables one has to iterate several times in such a way that these values represent the design of minimum weight. We note that a complete stress analysis of the structure has to be made during each iteration cycle. In order to cut down on the iteration time, it will be very necessary to make some simplifying assumption for the purpose of stress analysis. This is done in the next chapter in which a detailed formulation of the problem is given.

### III

#### ANALYSIS

##### 3.1 Formulation of the problem

The problem under consideration here, is that of optimization of a simply supported all composite corrugated hat stiffened panel under uniaxial compression. Figure (3) shows the panel under consideration. The material used in the analysis is graphite/epoxy.

##### 3.1.1 Basic assumptions

1. All the panel members are thin plates simply supported on all four edges.
2. All the panel members are orthotropic and have constant thickness.
3. Only three kinds of laminate orientations are used, namely  $0^\circ$ ,  $+45^\circ$ ,  $-45^\circ$ , relative to the axial direction.
4. Yield strain in compression for any panel member is equal to yield strain of  $0^\circ$  laminates irrespective of the percentage of  $0^\circ$  and  $+45^\circ$  laminates.
5. Each panel member is assumed to have only three layers.
6. Laminate layup in each panel member is assumed to be  $+45^\circ$ ,  $0^\circ$ ,  $+45^\circ$ .
7. Effect of Poisson's ratio is neglected in calculating the load carried by each panel member.

8. Panel is assumed to behave like a wide column for the purpose of Euler buckling analysis.

9. Torsional and local crippling failures of the panel modes are ignored.

### 3.1.2 Performance function

Under the assumption of wide column behavior only one pitch of the stiffener spacing is required for the purpose of further analysis. Figure (4) shows a representative cross-section of the panel.

The performance function in our analysis is a function of weight. It is chosen to be the weight per unit area per unit width of the panel.

$$\phi = \frac{\bar{\rho}A}{b} \quad (10)$$

### 3.1.3 Design Variables:-

Taking into consideration assumption (3), (5), and (6), the number of unknown design variables is reduced to twelve. They are (also see Figure 4)

1. Width of each panel member,  $b_i$
2. Thickness of each panel member,  $t_i$
3. Percentage of  $+45^\circ$  laminates in each panel member,  $f_i$

where  $i = 1, 2, 3, 4$

(11)

### 3.1.4 Constraints:

The panel must meet certain failure criterion and practical

requirements in order to be a valid design. They are as follows

1. Local buckling load of each panel member should be greater than or equal to the applied load.

$$P_{l_i} \geq P_{a_i} \quad (12)$$

2. Euler buckling load of the total panel should be greater than or equal to the applied loading,

$$N_{x_{\text{Euler}}} \geq N_{x_a} \quad (13)$$

3. Applied strain of the total panel should be less than or equal to cutoff, or yield strain.

$$\epsilon \leq \epsilon_y \quad (14)$$

4. Stiffner spacing should be greater than or equal to  $b_3$  (Figure 4)

$$b \geq b_3 \quad (15)$$

5. Value of design variables should be limited in a region of practical interest.

$$\left. \begin{aligned} b_i^L &\leq b_i \leq b_i^H \\ t_i^L &\leq t_i \leq t_i^H \\ f_i^L &\leq f_i \leq f_i^H \end{aligned} \right\} \quad (16)$$

For example, percentage of  $\pm 45^\circ$  laminates ( $f_i$ ) can not be less than zero and greater than hundred.

The value of all the above mentioned parameters are obtained through the use of a simplified stress analysis, as discussed below.

### 3.2 Stress Analysis

#### 3.2.1 Load in each panel member

Lets assume  $N_x$  is the load intensity per unit width,  $\sigma_{ai}$  is the axial stress in each panel member, and  $P$  is the total load per unit stiffner spacing. Now we can write

$$P = N_x \cdot b \quad (17)$$

and

$$P = \sum_{i=1}^4 \sigma_{ai} A_i \quad (18)$$

Because of compatibility considerations, the strain in each panel member has to be equal. Here we will neglect the effect of Poisson's ratio. Hence

$$\epsilon = \frac{\sigma_{ai}}{E_i} \quad i = 1, 2, 3, 4 \quad (19)$$

From Equations (18) and (19) we get

$$P = \sum_{i=1}^4 \epsilon E_i A_i$$

Solving this equation for the strain  $\epsilon$  and using Equation (17), we obtain

$$\epsilon = \frac{N_x b}{\sum_{i=1}^4 E_i A_i} \quad (20)$$

Finally the load  $P_{a_i}$  in each panel member is then given by

$$P_{a_i} = \sigma_{a_i} A_i = \frac{N_x b F_i A_i}{\sum_{i=1}^4 F_i A_i} \quad (21)$$

### 3.2.2 Local buckling

Each panel member is assumed to be orthotropic and simply supported on all four edges. Hence from orthotropic plate theory (reference 13), we can write

$$\sigma_l = \frac{2\pi^2}{b^2 t} (\sqrt{D_{11} D_{22}} + D_{12} + D_{66}) \quad (22a)$$

and

$$P_l = \sigma_l b t \quad (22b)$$

where,

$\sigma_{\ell}$  - is the local buckling stress

$b$  - is the width of the plate

$t$  - is the thickness of the plate

$D_{ij}$  - are the bending stiffness coefficients

$P_{\ell}$  - is the local buckling load

Here for the sake of simplicity subscript  $i$  has been omitted. However this equation applies to each panel member.

### 3.2.3 Euler buckling

We will consider one pitch of stiffner spacing for the purpose of Euler buckling analysis. Since each panel member can have different percentage of  $\pm 45^{\circ}$  laminates, each panel member is liable to have different value of Young's modulus. In order to find the Euler buckling load, we will use the equivalent area approach to find the effective Young's modulus and effective area of each panel member. Then we can employ

$$N_{x_{\text{Euler}}} = \frac{\pi^2 E_1 I}{b L^2} \quad (23)$$

In this expression  $E_1 \cdot I$  is the effective stiffness. Next we obtain  $I$ .

Let us assume

$y_i$  - distance of center of gravity of  $i^{\text{th}}$  panel member from reference axis (shown in Figure 4)

$E_i$  - Young's modulus for the  $i^{\text{th}}$  panel member

$A_i$  - Area of the  $i^{\text{th}}$  panel member

$\bar{y}$  - distance of the effective center of gravity of EA  
distribution from reference axis

so we can write

$$\bar{y} = \frac{\sum_{i=1}^4 E_i A_i y_i}{\sum_{i=1}^4 E_i A_i}$$

By dividing both the denominator and the numerator by  $E_1$ , we obtain

$$\bar{y} = \frac{\sum_{i=1}^4 \frac{E_i A_i}{E_1} y_i}{\sum_{i=1}^4 \frac{E_i A_i}{E_1}}$$

Let

$$A_i^* = \frac{A_i E_i}{E_1} \quad (24)$$

therefore

$$\bar{y} = \frac{\sum_{i=1}^4 A_i^* y_i}{\sum_{i=1}^4 A_i^*} \quad (25)$$

From Figure (4) we see that

$$\bar{b}_2 = \left[ \left\{ b_2 - \left( \frac{t_1 - t_4}{2} \right) \right\}^2 + \left( \frac{b_1 + b_3}{2} \right)^2 \right]^{1/2} \quad (26)$$

and

$$A_1^* = b_1 t_1$$

$$A_2^* = 2 \bar{b}_2 t_2 E_2 / E_1$$

(27)

$$A_3^* = b_3 t_3 E_3 / E_1$$

$$A_4^* = 2 b_4 (t_1 + t_4) E_4 / E_1$$

Hence

$$\bar{y} = \frac{A_2^* b_2 / 2 + A_3^* b_2 + A_4^* (t_1 + t_4) / 2}{(A_1^* + A_2^* + A_3^* + A_4^*)} \quad (28)$$

In order to find the moment of inertia about the center of gravity of the cross-section, we should adjust the effective width and the effective thickness of each panel member in such a way that the respective distance of the center of the gravity of each panel member should remain unaffected. For example, with reference to the figure (5) we note the width of the horizontal panel member has been modified, but not the thickness. However, for the inclined panel members, the thickness will be modified.

Hence we can define

$$b_3^* = A_3^* / t_3$$

$$b_4^* = A_4^* / t_4 \quad (29)$$

$$t_2^* = A_2^* / \bar{b}_2$$

Therefore, the moment of inertia  $I$ , is given by

$$\begin{aligned}
 I = & b_1 t_1^3 / 12 + b_4^* t_4^3 / 6 + b_3^* t_3^2 / 12 \\
 & + t_2^* \{b_2 - (t_1 + t_4) / 2\}^2 / 12 + A_2^* (\bar{y} - b_2 / 2)^2 \\
 & + A_3^* (\bar{y} - b_2)^2 + A_1^* \bar{y}^2 + A_4^* \{\bar{y} - (t_1 + t_2) / 2\}^2 \quad (30)
 \end{aligned}$$

### 3.3 Discussion of minimization procedure

At this point it is noted that the standard weight strength parameters are  $N_x/L$  and the weight per unit area per unit length ( $W/bL^2$ ) (Reference 7). The length of the panel is not by itself a design parameter. In the present analysis, we will assume that the loading  $N_x$  and length  $L$ , of the panel are known design parameters. However it will be shown in the optimization process that this approach will lead to the same weight strength plot. That is,  $N_x/L$  is indeed the pertinent parameter, and not  $N_x$  and  $L$  separately.

In order to minimize the weight function of equation (10), it will be necessary that all the constraints of equation (12) through (16), be satisfied. After satisfying all the constraints and reaching a minimum solution, the outcome of the analysis will be the extremizing values of design variables of equation (11). For the purpose of reaching a minimum solution, an optimization computer program AESOP is used (see appendix A and Reference 9).

It is very important to check the effects of the simplifying

assumptions. For this purpose another existing computer program BUCLASP-2 is used. (See appendix B and Reference 10). This program is capable of performing the buckling analysis of a biaxially loaded composite panel. A short description of the assumptions made in BUCLASP-2 analysis and the mathematical model required for the purpose of analysis is presented in Appendix-B. It should be noted at this point that BUCLASP-2 is not used as an optimization program, but it is used to predict the buckling loads of an optimized panel.

## IV

### NUMERICAL RESULTS

In the present work following two cases of hat stiffened panels under uniaxial compression have been optimized using "AESOP".

1. All-aluminum panel
2. All-composite (Graphite/Epoxy) panel

The material properties used for the purpose of analysis are presented in Table (1).

Tables (2) through (7) give the values of optimized design variables for various loading conditions and length of minimum weight Graphite/Epoxy panel. The values of the design variables for various loadings and length of the minimum weight aluminum panels are shown in Table (8).

Tables (1) through (3) show the values of weight per unit area per unit length ( $W/bL^2$ ) and axial load per unit length per unit width ( $N_x/L$ ) for different lengths of the panel. It can be seen that for same value of  $N_x/L$  the corresponding value of  $W/bL^2$  is similar in all three cases. This proves that  $N_x$  and  $L$  do not have to be considered separately but only  $N_x/L$  should be considered while obtaining these plots.

Figure (6) shows a standard weight strength plot for a composite and an all aluminum panel under uniaxial compression. In Figure (6),  $N_x/L$  is the load per unit width per unit length, and  $W/bL^2$  represents the weight of the panel per unit area per unit length.

Results of Reference (2) and the results obtained through the use of BUCLASP-2 (Reference 10) are also presented in Figure (6) for the purpose of comparison. For the all aluminum panel, a comparison was made with the results obtained by Crawford and Burns (Reference 2). As may be seen from figure (6), the present results show a slight weight advantage over the results obtained in Reference (2). This may be due to the fact that in the present analysis no assumption was made with respect to the cross-sectional dimensions of the panel. It is also noted that Reference (2) uses the condition that for minimum weight, the local buckling stress in each panel member is set equal to the Euler buckling stress of the whole panel. In the present analysis no such condition for minimum weight design was imposed. However it is interesting to note that the results obtained after minimization process showed that in fact for minimum weight, local buckling and Euler buckling stresses should be equal in each panel member.

For all composite panels an attempt was made to make a comparison with available optimization results. Unfortunately, the author was unable to find such results. So instead, a comparison was made to study the effects of simplifying assumption employed in the present stress analysis. This was done by determining the buckling load for the optimum panel by using the BUCLASP-2 computer program, which is devoid of such assumptions. A comparison was then made between the buckling load obtained by BUCLASP-2 for the optimum panel and the specified load, that was used in the present analysis to obtain the optimum panel. Figure (6) shows good correlation between the present results and those obtained through the use of BUCLASP-2.

The advantage of employing simplified stress analysis is, that it results in very small computational time. For example, with the use of the simplified stress analysis, the runtime for 1500 iteration is about four seconds on the CDC-6600 computer. It is interesting to note that even for all composite panels, the results obtained through the use of BUCLASP-2 show that the local buckling load and Euler buckling load of optimized panels is very close to each other.

Examination of Figure (6) reveals that all composite panels weigh approximately half as much as all aluminum panels. This result for all composite panels is very useful for modern aircraft technology. It is hoped that the results of this study will lead to further investigation in the use of composite materials for various design problems.

Figure (7a) and (7b) show that there are two different design possible for the same loading condition Figure (7a) pertains to a lightly loaded panel ( $N_x/L = 50$ ) whereas figure (7b) applies to a heavily loaded panel ( $N_x/L = 500$ ). For each loading case, both of the designs weigh almost the same (see Tables 2 and 5), but both have different values of design variables. This phenomenon allows for more flexibility during the design process and less weight penalties will be felt if practical constraints (e.g. manufacturing restrictions) are imposed on such panels. However one should make sure in such cases of multiple optimum designs, that these designs are not the result of the various assumptions made during the stress analysis. Figure (8) shows the buckling mode shapes for the two highly loaded panels (Figure 7b). These mode shapes were obtained

from BUCLASP-2. The panel in Figure (8a) is very deep as compared to its width and fails in a torsional mode. Since the torsional mode of failure was neglected in the stress analysis of the given panel, this panel is not a valid design, and can be ignored. The panel in Figure (8b) fails in a local buckling mode, such that all the panel members behave almost simply supported, which is in accord with one of the simplifying assumption.

We note the panel on the bottom of Figure (7) have one hundred percentage  $+45^{\circ}$  laminates in the skin and in the inclined panel members. Also the thickness of the inclined members and skin is very small compared to the thickness of other panel members (See Tables 2-7). This suggests that most of the load is carried by  $0^{\circ}$  filaments, which is desirable in order to have most efficient panel. At this point it should be noted that under such condition neglectation of the effect of Poisson's ratio is a good assumption. Recall that this assumption was made in the calculation of the axial load carried by each panel member. These panels also verify a very useful concept of reinforcing hat stiffened metallic panels. In reinforcing such panels strong load carrying material is added in the direction of the loading. For example, the reinforcement is added along the flanges and the skin connections in case of hat stiffened panels.

Finally, it is noted that some of the assumptions made in the analysis of these panels did not effect the results to any significant amount. These assumptions are discussed next.

1. The yield strain assumed to be that of all  $0^{\circ}$  filaments is considered to be a good assumption because most of the load is carried by  $0^{\circ}$  filaments.

2. Laminating layup in each panel member turned out to be of no importance, because all the panel members have only one kind of laminate orientation, i.e.  $\pm 45^\circ$  or  $0^\circ$ , and never have both  $0^\circ$  and  $\pm 45^\circ$  filaments orientation.

CONCLUDING REMARKS

In the present work an attempt has been made to discover some of the new concepts in the optimum design of structural members, composed of composite materials. Since there are no available results for the purpose of comparison, it will be very desirable to carry out experimental verification of the results obtained in the present analysis. It should be noted that the results obtained in the present analysis are optimums but are not very practical. For example, it is not desirable to have all  $0^\circ$  filaments in any of the panel members. The imposition of such practical constraints will result in a heavier panel. If instead, however, the design variables are chosen in such a way that an optimum design includes the practical constraints, relatively lighter practical designs may be found.

For the case considered herein, the present analysis shows that composite panels are approximately twice as light as all aluminum panels. It is hoped that this result will inspire further investigations into the use of composites for optimum designs. In the present analysis some of the assumptions were very crude and need to be modified. For example, the yield strain for the whole panel was assumed to be equal to yield strain of all  $0^\circ$  filaments. This assumption in the present analysis did not effect the design to any significant amount, because most of the load is carried by  $0^\circ$  filaments. However this will not be true in general. This suggests a more general yield criteria is required. Furthermore it will be interesting to investigate panels with different geometry, boundary conditions and loading conditions.

## REFERENCES

1. Michell, A. G. M., "The limits of economy of material in frame structures," *Phil. Mag.* 8, (1904).
2. Crawford, R. F., and Burns, A. B., "Minimum weight potentials for stiffened plates and shells," *AIAA Journal* Vol. 1, No. 4, (1963).
3. Becker, H., "The optimum proportions of a multicell box beam in pure bending," *J. Roy. Aeronau. Soc.*, 16, (1949).
4. Becker, H., "The optimum proportions of a long unstiffened circular cylinder in pure bending," *J. Aeronau. Sci.* 15 (1948).
5. Zahorski, A., "Effects of material distribution on strength of panels," *J. Aeronau. Sci.* 2, 247-253 (1949).
6. Farrar, D. J., "The design of compression structures for minimum weight," *J. Roy. Aeronau. Soc.* 53, 1041-1052 (1949).
7. Shanley, F. R., "Weight strength analysis of aircraft structures (McGraw-Hill Book Co.) N. Y., 1952.
8. Gerard, G., "Efficiency applications of stringer panel and multicell wing construction," *J. Aeronau. Sci.* 15, 616-624 (1948).
9. Jones, R. T. and Hague, D. S. "Applications of multivariable search techniques to structural design optimization," NASA CR-2038, June (1972).
10. Tripp, Leonard L., Tamekuni, M., Viswanathan, A. V., "A computer program for instability analysis of biaxially loaded composite stiffened panels and other structures," User's manual for "BUCLASP-2", "NASA CR-112226, 1973.
11. Gerard, G., "Minimum weight analysis of compression structures", (N.Y.U. Press, New York, 1956).
12. Bryson, A. E., and Denham, W. F., "A steepest-ascent method for solving optimum programming problems," Raytheon Report, BR-1303.
13. Timoshenko, S., "Theory of elastic stability (McGraw-Hill Book Co., New York, 1936).
14. Cox, H. L. and Smith, H. E., "Structures of minimum weight," Aeronau. Research Council, R M 1923 (Nov. 1943).

15. Schuette, E. H., "Charts for the minimum weight design of 24 S-T aluminum-alloy flat compression panels with longitudinal Z-section stiffeners," NACA TR 827 (1945).
16. Anderson, M. S. "Local instability of the elements of a trusscore sandwich plate," NASA TR R30 (1959).
17. Seide, P., and Stein, M., "Compressive buckling of simply supported plates with longitudinal stiffeners," NACA TN-1825 (1949).
18. Gerard, G., "Optimum structural design concepts for aerospace vehicles", AIAA J. Vol. 3, No. 1, (Jan. 1966).
19. Morrow, M. W. and Schmit, L. A. Jr., "Structural synthesis of a stiffened cylinder," NASA CR-1217 (Dec., 1968).
20. Hague, D. S., "Atmospheric and near planet trajectory optimization by the variational steepest-descent method, NASA CR-73366, 1969.
21. Wilde, D. J. "Optimal seeking methods," Prentice-Hall, 1964.
22. Fox, Richard L., "Optimization methods for Engineering design". Reading Mass., (Addison-Wesley Publishing Co. 1971).

## APPENDIX A

### Optimization Technique

This appendix is presented here for the sake of completeness. The contents of this appendix are available in reference (9). In this appendix techniques available in AESOP, for the solution of non-linear multivariable optimization problems are discussed. A wide variety of search algorithms have been devised for the solution of multivariable optimization problems. Many of these algorithms are restricted to the solution of linear or quadratic problems. Algorithms of this type must be supplemented by more general search procedures if generality of solution is sought. This is because engineering problems tend to lead to non-linear formulation with the possibility of discontinuities in both the performance function response surface and its derivative. Most of the searches which prove effective in these problems combine a direction generating algorithm, such as steepest-descent, with a one-dimensional search. Distance traversed through the control space in the selected direction is measured by a step-size, or perturbation parameter DP. The object of the one-dimensional search is to determine the value of DP which minimizes the performance function along the chosen ray and to establish the corresponding control vector.

In practice, the diverse nature of non-linear multi-variable optimization problems leads to the conclusion that no one search algorithm can be uniquely described as being the "best" in all the situations which may be encountered. Rather, a combination of searches, some of which may be of quite elementary nature, provides the most reliable and economical convergence to the optimal solution.

One dimensional search: Multivariable search problems are reduced to one-dimensional problems whenever a search algorithm is used to establish a one-to-one correspondence between the control vector and a single scalar perturbation parameter, DP. In such a situation

$$\alpha_i = \alpha_i(DP), i = 1, 2, \dots, N \quad (A1)$$

so that equation (2) becomes

$$\phi = \phi(\alpha_i) = \phi(DP) \quad (A2)$$

Similarly, the right hand sides of equation (3) and (7) become functions of the scalar perturbation parameter.

The relationship, equation (A1), specifies a ray through the control space. As noted above, the objective of the one-dimensional search along this ray is to locate the value of DP which provides the minimum performance function value.

Numerical search for the one-dimensional minima can be carried out in a local fashion, by the Newton-Raphson method, for example, or by a global search of the ray throughout the feasible region. The localized polynomial approximation is appropriate to the terminal convergence phase in a problem solution when some knowledge of the extremal's position has been accumulated by the preceding portion of the search and the problem involves a smooth function. The global search can be used to advantage in the opening moves of a search. In the early phase of a search the object is to isolate the approximate neighborhood of the minimum performance

function value as rapidly as possible, usually with little or no fore-knowledge of the performance function behavior. One measure of the effectiveness of a search algorithm in such a situation is the number of evaluations required to locate the minimum point to some prespecified accuracy. It can be shown that the most effective method of locating the minimum point of a general unimodal function is a Fibonacci search (reference 21). In this method, the accuracy to which the minimum is to be located along the perturbation parameter axis must be selected prior to the commencement of the search. Since the accuracy required is highly dependent of the behavior of the performance function, this quantity is difficult to prespecify.

Prespecification of the accuracy to which the extremal's position is to be located can be avoided for little loss in search efficiency by use of an alternative search based on the so-called golden section. (reference 21). This is the method employed in the AESOP code one-dimensional search procedure. Search by the golden section commences with the evaluation of the performance function at each end of the search interval and at  $G = 2/(1 + \sqrt{5})$  of the search interval from both of these bounding points. This is illustrated in figure (A1).

The boundary point furthest from the lowest resulting performance function value is discarded. The three remaining points are retained, and the search continues in a region which is diminished in size by  $G$ . The internal point at which the performance function is known in the reduced interval will be at a distance  $G$  of the reduced interval from the remaining bounding point of the original interval for  $(1-G) = G^2$ . The

search can, therefore, be continued in the reduced interval with a single additional evaluation of the performance function. It follows after  $Q$  evaluations of the performance function that the position of the extremal point will be known within  $R$  of the original search region where

$$R = G^{(Q-3)} \quad (A3)$$

To reduce the interval of uncertainty to .00001 of the original search interval, about 27 evaluations of the performance function are required. For a reasonable number of evaluations of the performance function, this type of search is almost as efficient as a Fibonacci search.

It should be noted that search by the golden section proceeds under the assumption of unimodality; hence it will often fail to detect the presence of more than one minimum when the performance function is multimodal. If more than one minimum does exist, the one located depends on performance behavior within the original search interval.

Multiple Extremals on a One-Dimensional Ray: The one-dimensional section search described above is unable to distinguish one local extremal from another; it will merely find one local extremal. This difficulty can be largely eliminated by the addition of some logic to the search, at least for moderately well behaved performance functions; that is, for functions having a limited number of extremals in the control space region of interest. An effective method for detecting multiple extremals is to combine the one-dimensional search with a

random one-dimensional search on the same ray through the control space. This is illustrated in figures A2 and A3. In Figure A2 the response contours of a performance function having two minima are illustrated together with the initial points used in a global one-dimensional search by the golden section method. The behavior of the function at these points is shown in figure A4 A3. The left hand minimum is not apparent from these points. If a single random point is added in the interval  $L_0$ , the probability of this point revealing the presence of the second minimum is

$$P_1 = L_1/L_0 \quad (A4)$$

for any point in the interval AB indicates the presence of a local minimum somewhere in the interval AB, and any point in the interval BC indicates the presence of a local maximum somewhere in the interval BC. In this latter case, there must be a minimum of the function both to the left and to the right of the newly introduced point.

If random uniformly distributed points are added in the interval  $L_0$ , the probability of locating the presence of the second minimum becomes

$$P_R = 1.0 - (1.0 - L_1/L_0)^R \quad (A5)$$

The function  $(L_1/L_0)$  is a measure of the performance function behavior. For a given value of this behavior function the number of random points which must be added to the one-dimensional search to provide a given probability of locating a second minimum can be determined.

The presence of multiple minima on a one-dimensional cut through an N-dimensional space does not necessarily indicate that the performance function possesses more than one minimum in a multi-dimensional sense. It may be that the performance function is merely non-convex. This is illustrated by figure A4. The performance function behavior on the one-dimensional search in figures A2 and A4 is identical. In figure A2 this indicates the presence of two local extremals; in figure A4, a non-convex performance function.

When a one-dimensional search detects the presence of multiple extremals in the local sense above, a decision must be made as to which of the apparent extremals is to be pursued during the remainder of the search. Here, without foreknowledge of the performance function behavior, logic must suffice. Typically, the left or right hand extremal, the extremal which results in the best performance, or even a random choice may be made.

It should be noted that logic of this type is not currently available in the AESOP code. The AESOP one-dimensional search procedure has three distinctive phases. First, each search algorithm defines an initial perturbation using either past perturbation stepsize information or a perturbation magnitude prediction as in the quadratic search (Reference 9). Second, a perturbation stepsize doubling procedure is employed until a point exhibiting diminishing performance is generated. Third, having coarsely defined the one-dimensional extremal position from steps one and/or two, a golden section search is employed to locate the extremal with reasonable precision.

Multiple extremals - general procedure: The multiple extremal search technique included in AESOP is based on topologically invariant warping of the performance response surface. The response surface is warped in a manner which retains all the surface extremals but alters their relative locations and regions of influence. The regions of influence of an extremal is defined as the hull or collection of all points which lead to the extremal if a gradient path is followed. Reducing the region of influence of an extremal decreases the probability of locating a point in the neighborhood of the extremal if points are chosen at random. Again, in an organized multivariable search, the probability of locating an extremal having a small region of influence is less than that of locating an extremal having a large region of influence. For example, suppose the extremals of the one-dimensional function of figure A5 are to be determined in the range  $\alpha_L < \alpha < \alpha_H$  by the sectioning approach. The four initial values employed in this technique are denoted by  $f_1$  to  $f_4$ .

Following evaluation at these four points,  $f_4$  is discarded, and the function is evaluated at  $f_5$ . At this point the right-hand extremal,  $e_2$ , has been eliminated from the search which now inevitably proceeds to the left hand extremal at  $e_1$ .

To find the second extremal, the function  $F$  is warped by writing

$$F(\xi) = F(\alpha)$$

$$\xi = (\alpha_H - \alpha^*) \left[ \frac{\alpha - \alpha^*}{\alpha_H - \alpha^*} \right]^{2N} + \alpha^*; \quad \alpha > \alpha^* \quad (A6)$$

$$\xi = -(\alpha^4 - \alpha_L) \left[ \frac{\alpha^* - \alpha}{\alpha^* - \alpha_L} \right]^{2N} + \alpha^*; \quad \alpha^* > \alpha \quad (A7)$$

where  $N$  is a positive integer, and  $\alpha^*$  is the location of the left hand extremal.

A typical relationship between  $\xi$  and  $\alpha$  is shown in figure (A6) for the case  $N = 1$ . Differentiation of equation A7 with respect to  $\alpha$  when  $N = 1$  results in

$$\xi^1 = \frac{2[\alpha - \alpha^*]}{[\alpha_H - \alpha^*]} ; \alpha \geq \alpha^* \quad (A8)$$

$$\xi^1 = \frac{2[\alpha^* - \alpha]}{\alpha^* - \alpha_L} ; \alpha < \alpha^*$$

Note that as  $\alpha \rightarrow \alpha^*$ ,  $\xi^1 \rightarrow 0$  from both the left and right. At  $\alpha = \alpha_L$  and at  $\alpha = \alpha_H$ ,  $\xi^1 = 2$ . In the regions  $\alpha_L < \alpha < \alpha^*$  and  $\alpha^* < \alpha < \alpha_H$   $\xi$  varies parabolically with  $\alpha$ . Figure A7 illustrates these points. It can be seen that a region  $\Delta\alpha_1$  centered about  $\alpha^*$  transforms into a smaller region  $\Delta\xi_1$  located in the neighborhood of  $\xi = \alpha^*$ . On the other hand, a region  $\Delta\alpha_2$  situated in the neighborhood of the upper search limit, maps into a wider region in the neighborhood of  $\xi = \alpha_H$ . In general, the slopes at  $\alpha = \alpha_L$  and  $\alpha = \alpha_H$  are given by  $2N$ ; the greater the  $N$ , greater the warping becomes.

The effect of introducing a moderate warping transformation on the function of figure (A5) is shown in figure (A7). It can be seen from figure (A7) that the region of influence of  $e_1$  is reduced, and the region of influence of  $e_2$  is increased. On the warped surface search by sectioning commences with the evaluations of performance at  $\bar{f}_1$  to  $\bar{f}_4$ . Following these initial evaluations  $\bar{f}_1$  is discarded (as opposed to the



## APPENDIX - B

### BUCLASP-2 Assumptions and Model

This appendix is devoted to a discussion of some of the capabilities of BUCLASP-2 (A Computer Program for the Instability Analysis of Biaxially Loaded Composite Panels) as it pertains to the buckling analysis of the composite panels considered in the present work. This computer program (reference 10) is operational on the CDC-6600 computer. It is quite reliable and gives very good results for the buckling problems of composite panels. Some of the basic assumptions made in the analysis of BUCLASP-2 are as follows:

1. The panel members are orthotropic
2. The material is linearly elastic
3. Thin plate theory is employed
4. Effects of prebuckling deformations are ignored
5. Eccentricity effects are accounted for
6. Exterior edges in planes normal to the prismatic direction are assumed to be simply supported.

Support conditions at other boundaries are arbitrary. With the above assumptions an "exact" analysis of the whole panel is made. This analysis results in the prediction of Euler buckling modes, local buckling modes, or coupled Euler and, local modes.

The user of BUCLASP-2 has to define the mathematical model of the panel under consideration. This mathematical model consists of three substructures, namely the start substructure, end substructure, and the repeat substructure. Figure B1 shows the cross sections of the three

substructures for the panel studied in this investigation.

The results after using AESOP define the cross-sectional dimensions of the panel. These dimensions are used to find the buckling load using BUCLASP-2.

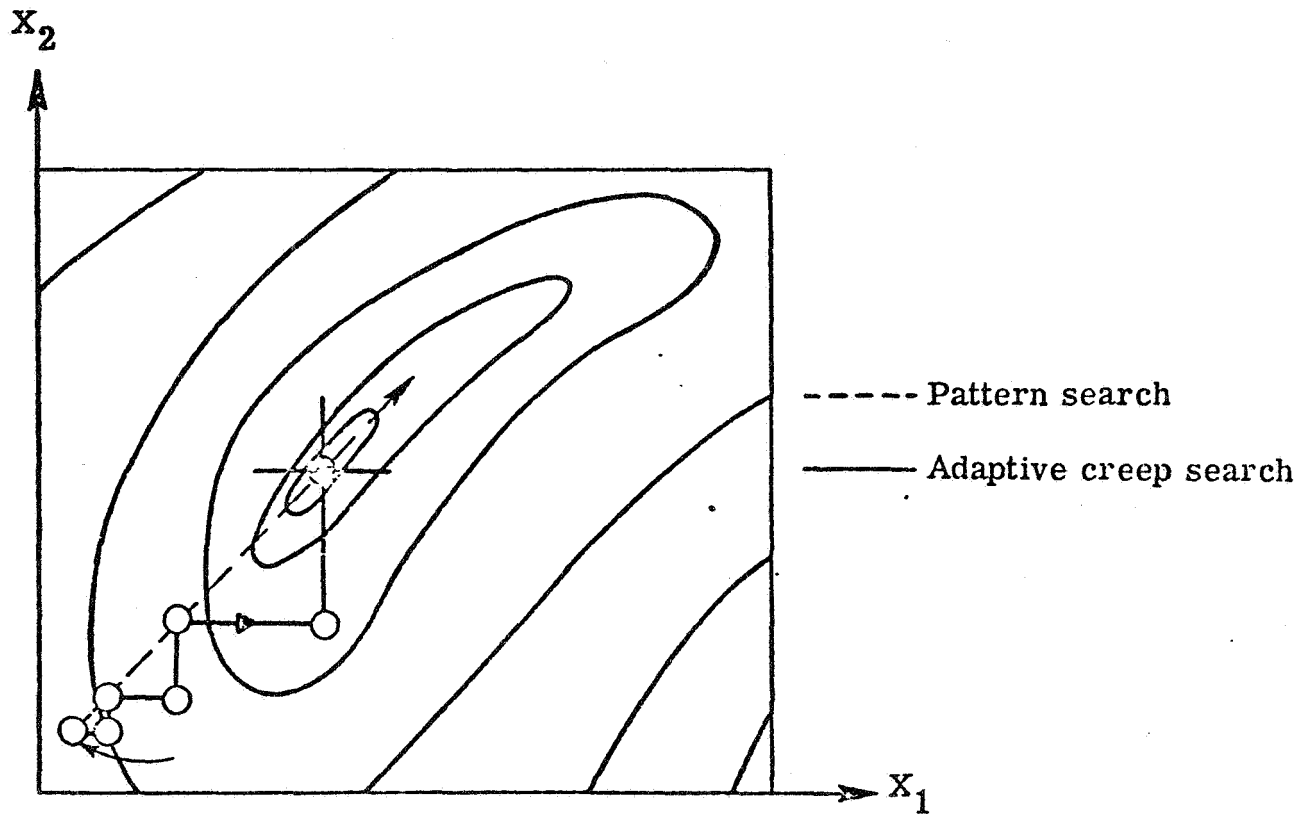


Figure 1.- Search processes.

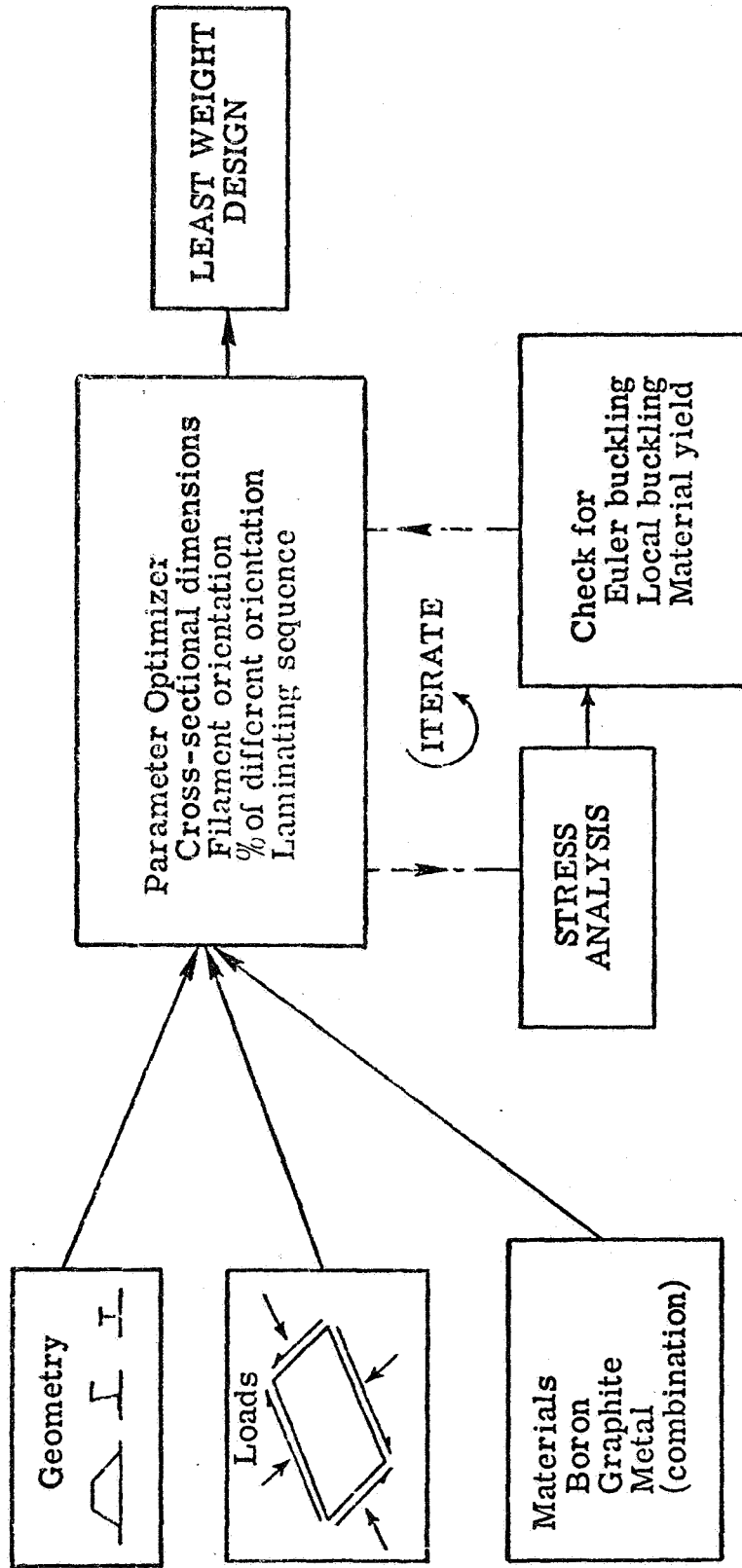


Figure 2.- Optimization cycle.

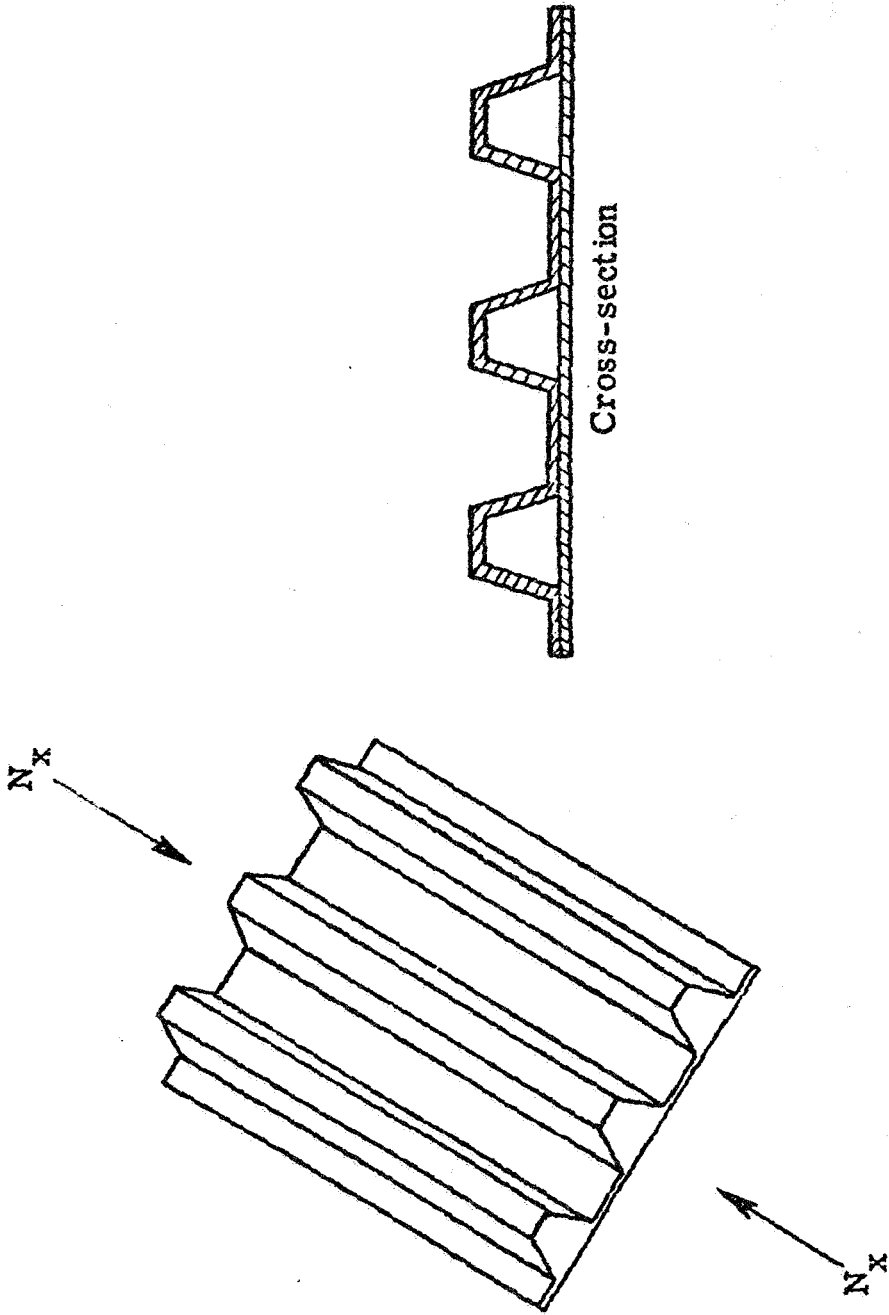


Figure 3.- Panel to be optimized.

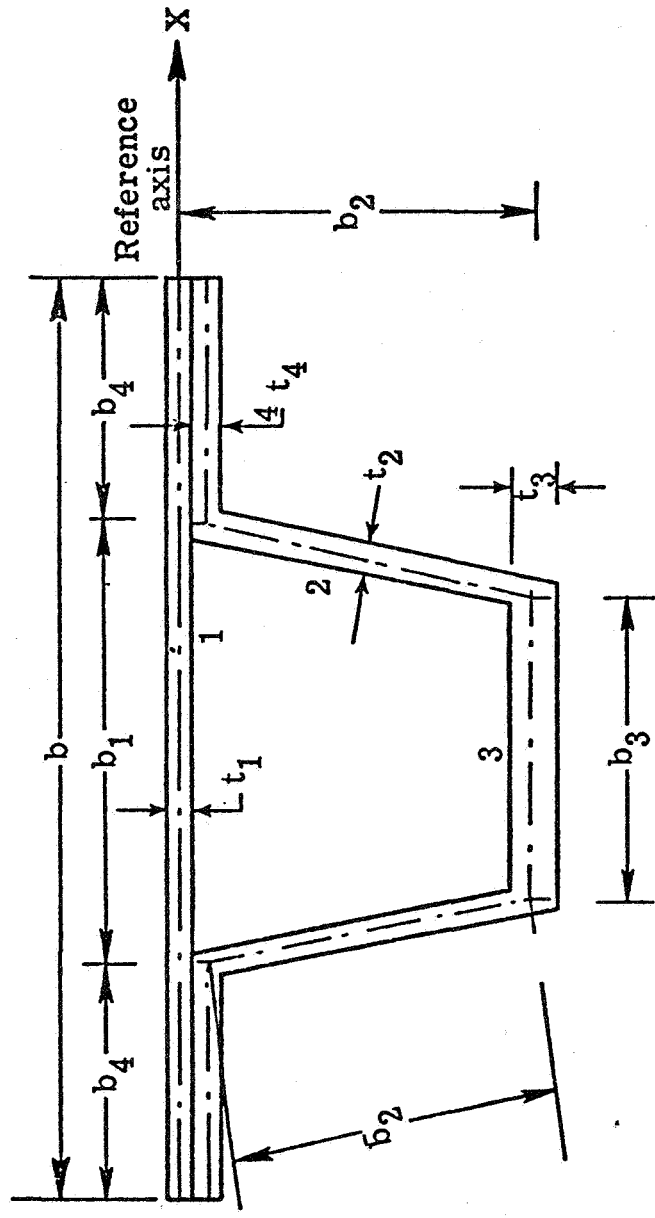


Figure 4.- Representative cross-section of the panel.

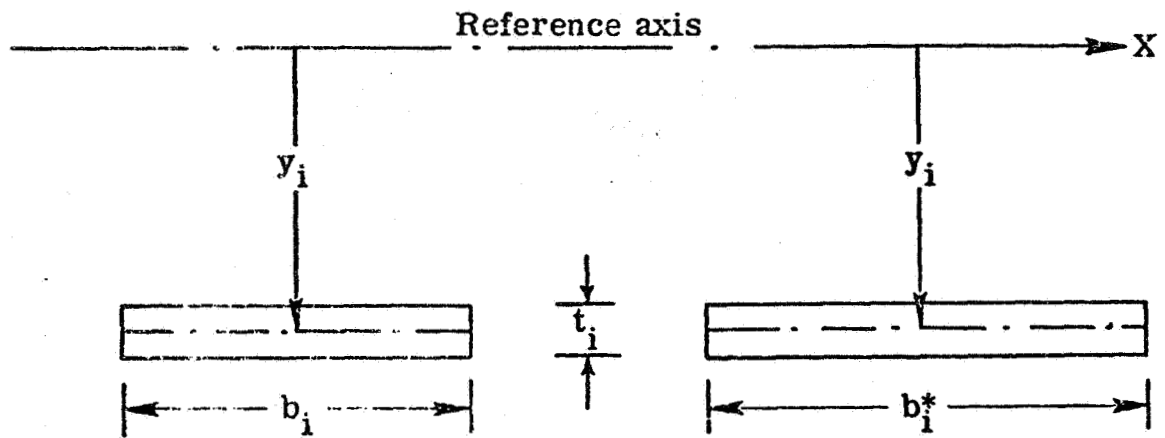


Figure 5.- Equivalent width.

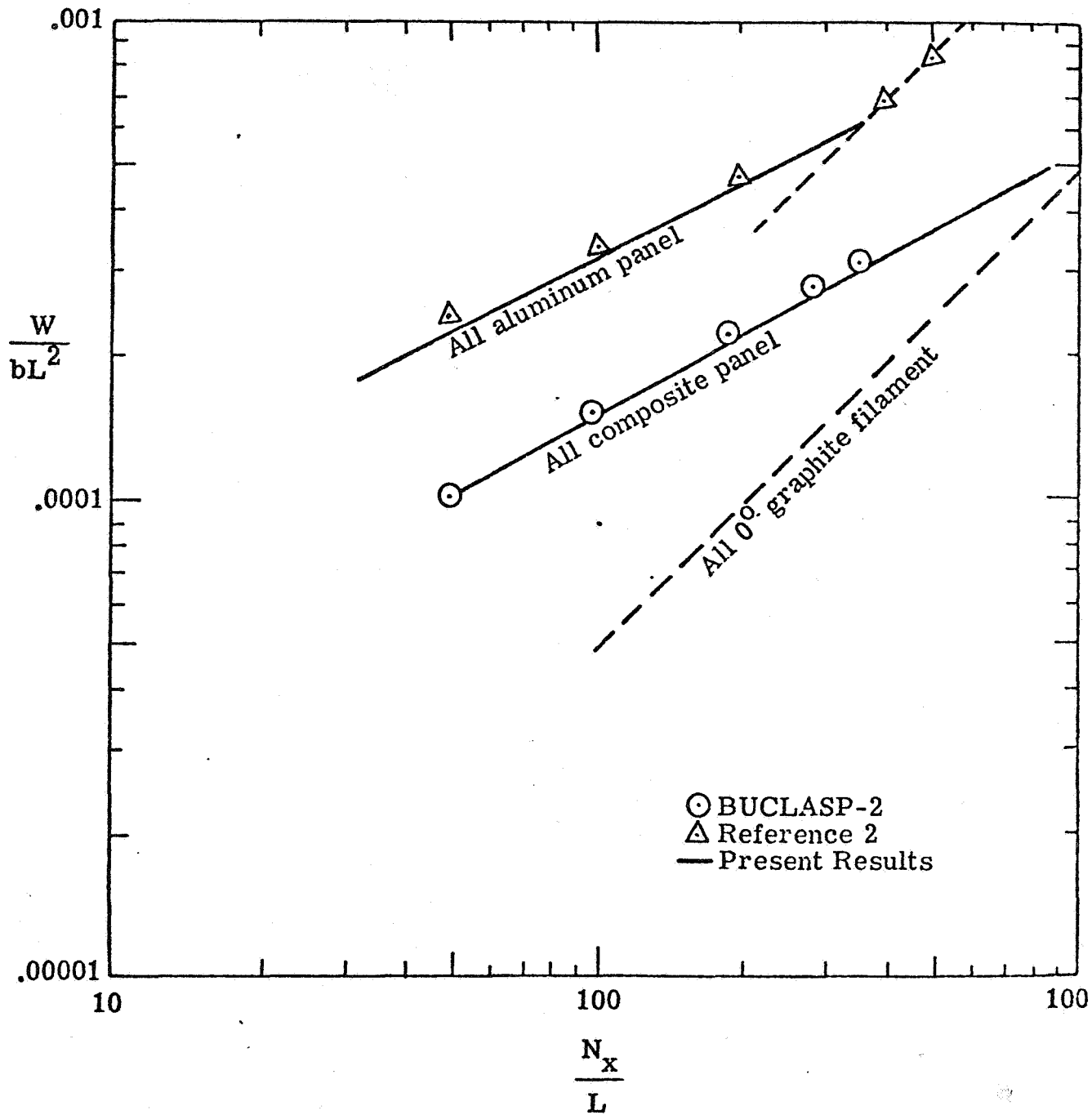


Figure 6.- Weight strength plot for all-composite and all-aluminum panels.

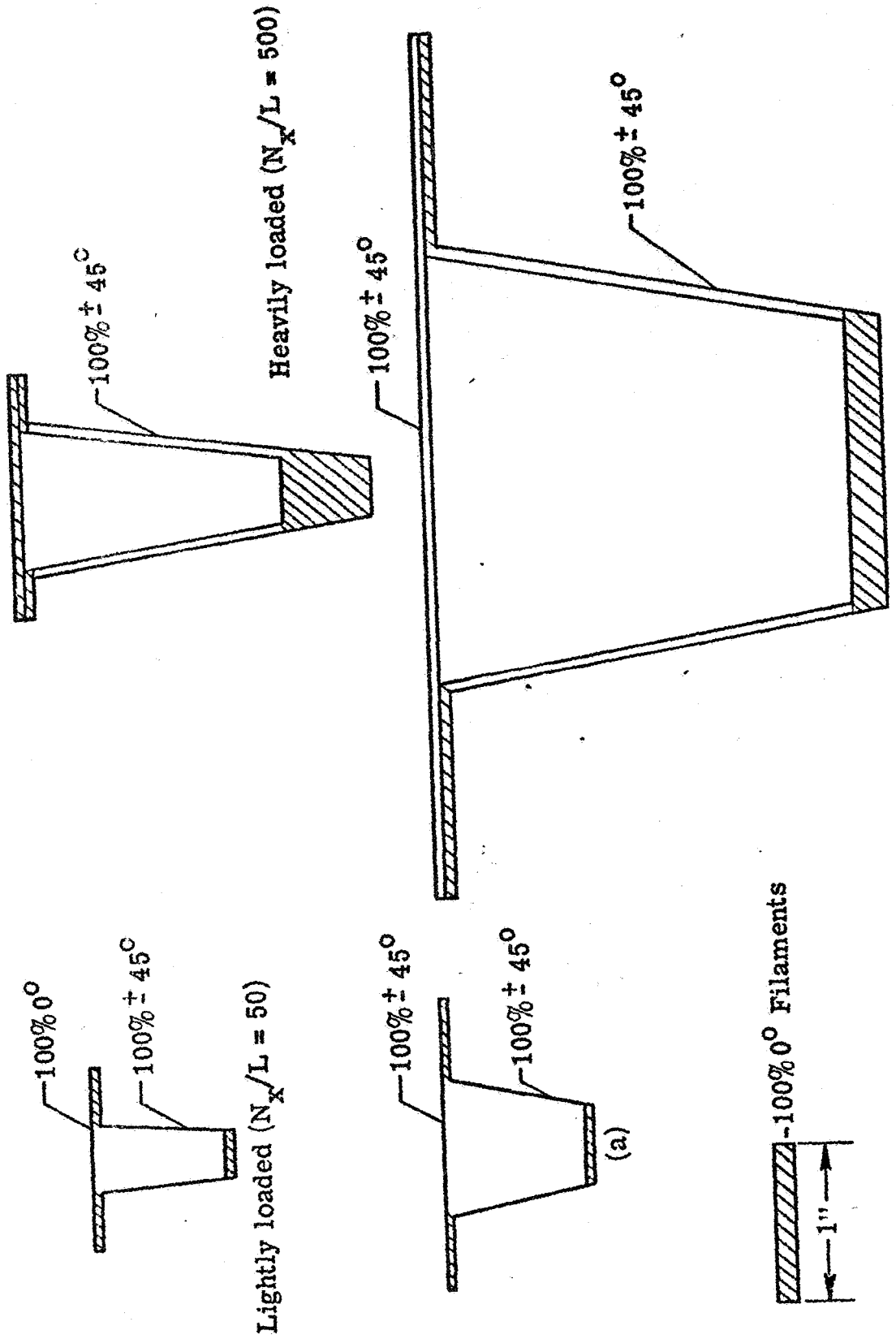


Figure 7- Optimized Sections (Full scale)

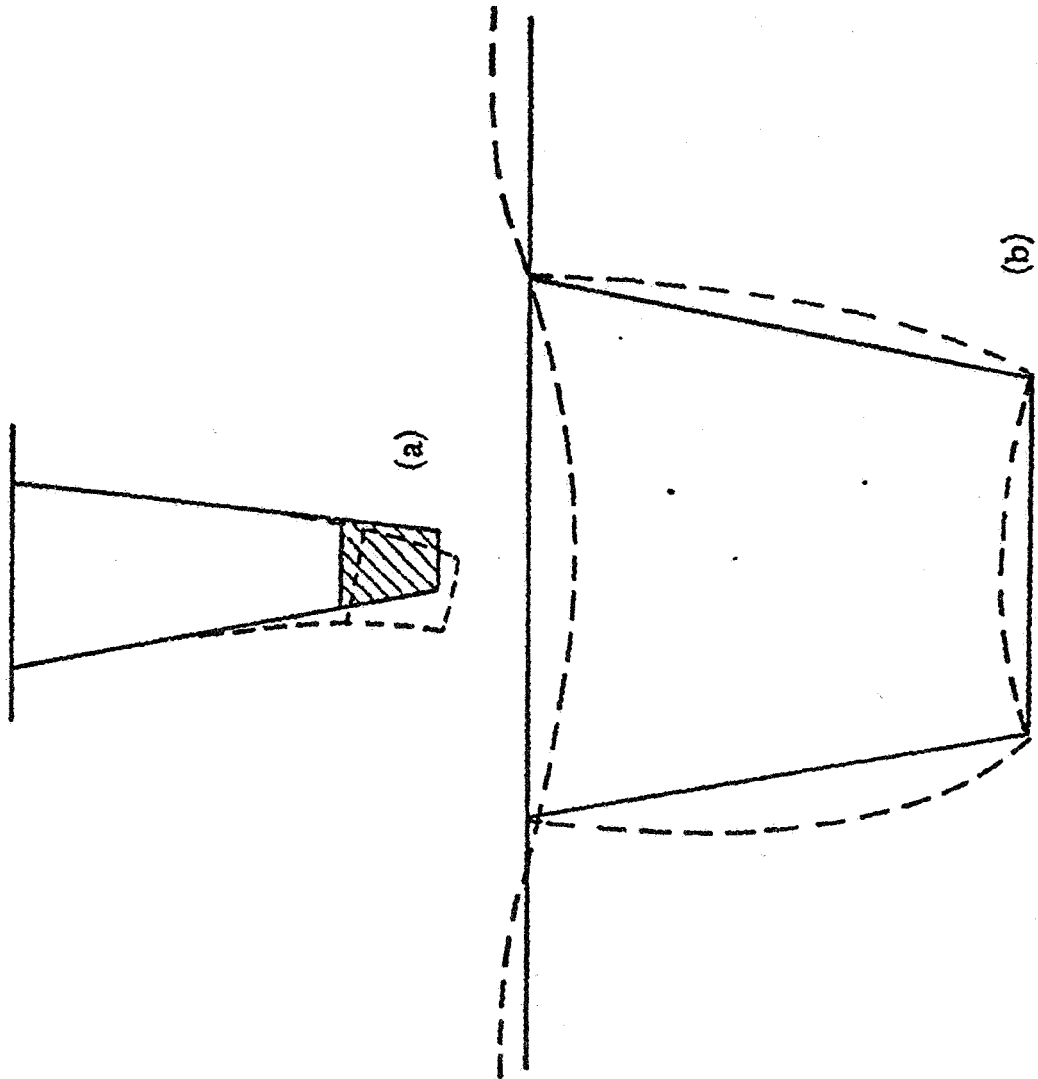


Figure 8.- Buckling modes.

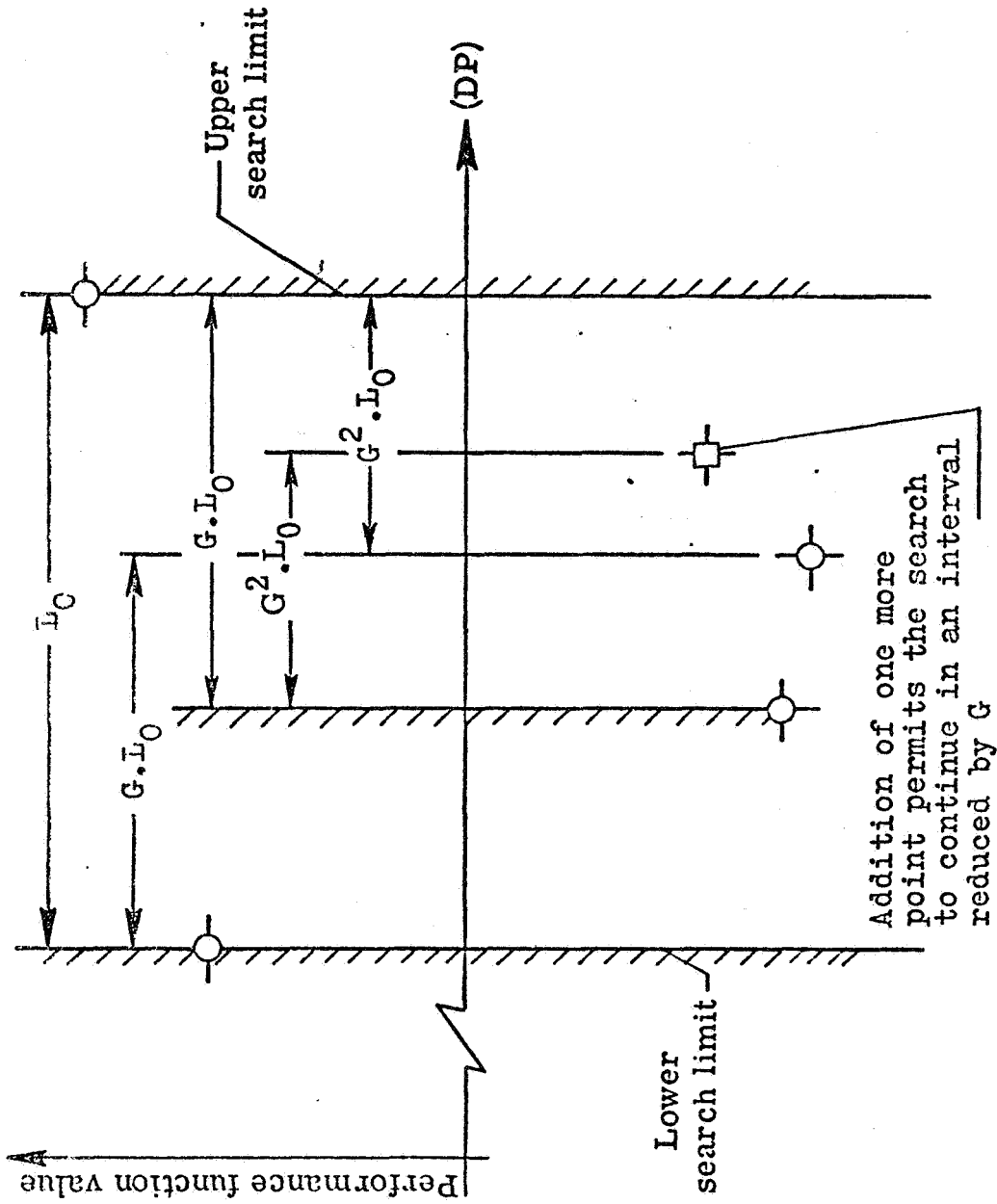


Figure A1.- Search based on Golden section.

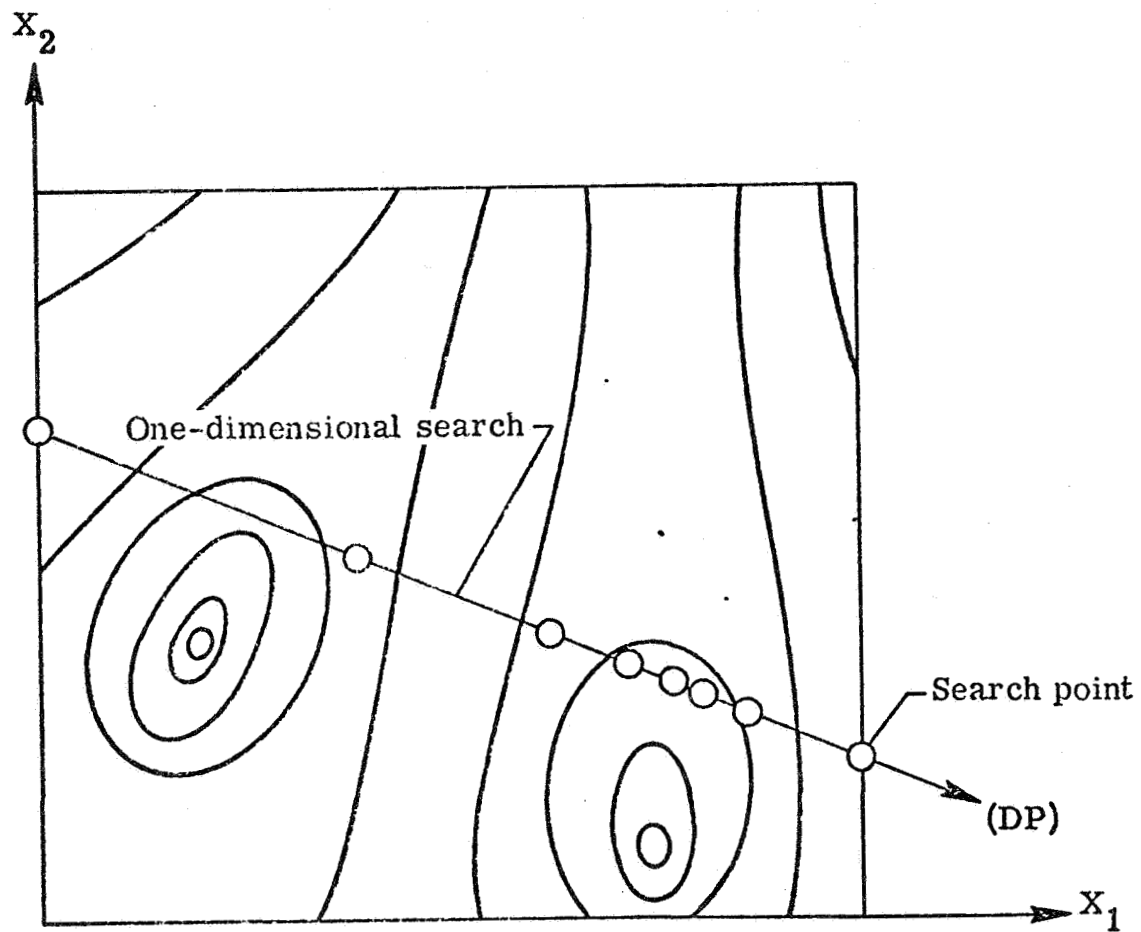


Figure A2.- Response surface with two troughs.

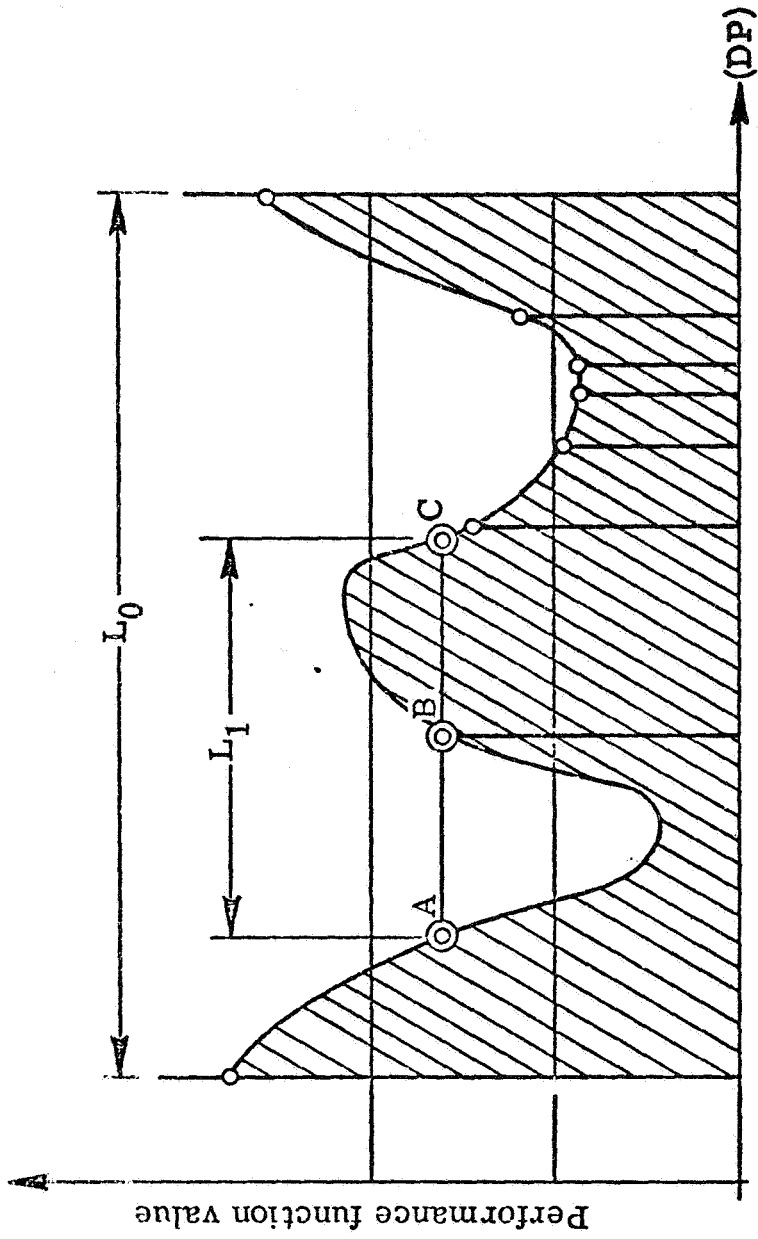


Figure A3.- Search by Golden section fails to detect multiple troughs on one-dimensional cut.

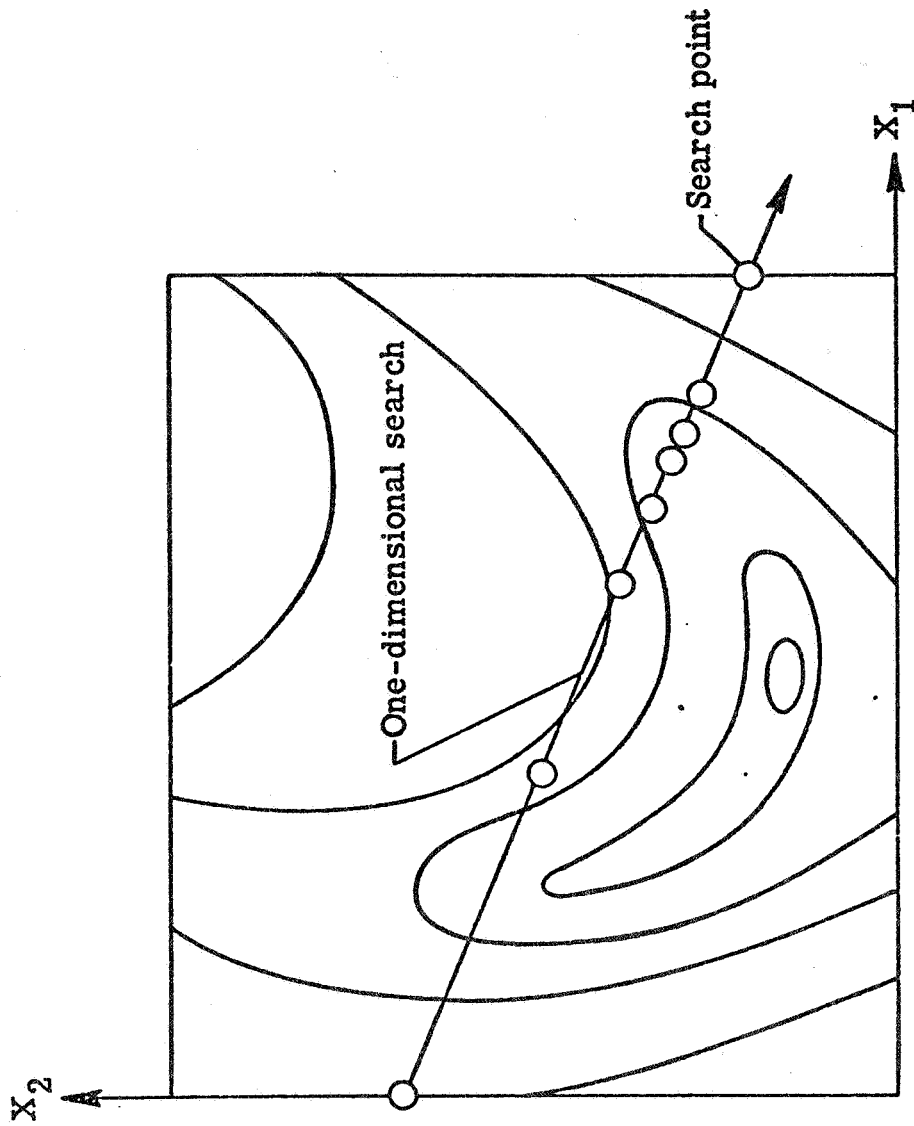


Figure A4.- Non-convex response surface.

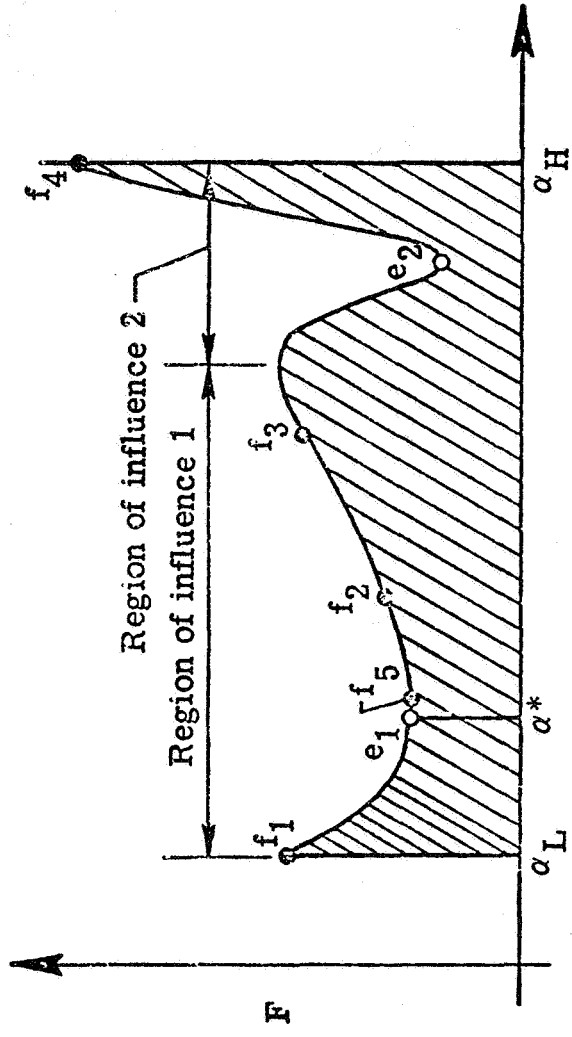


Figure A5.- Function with two extremes.

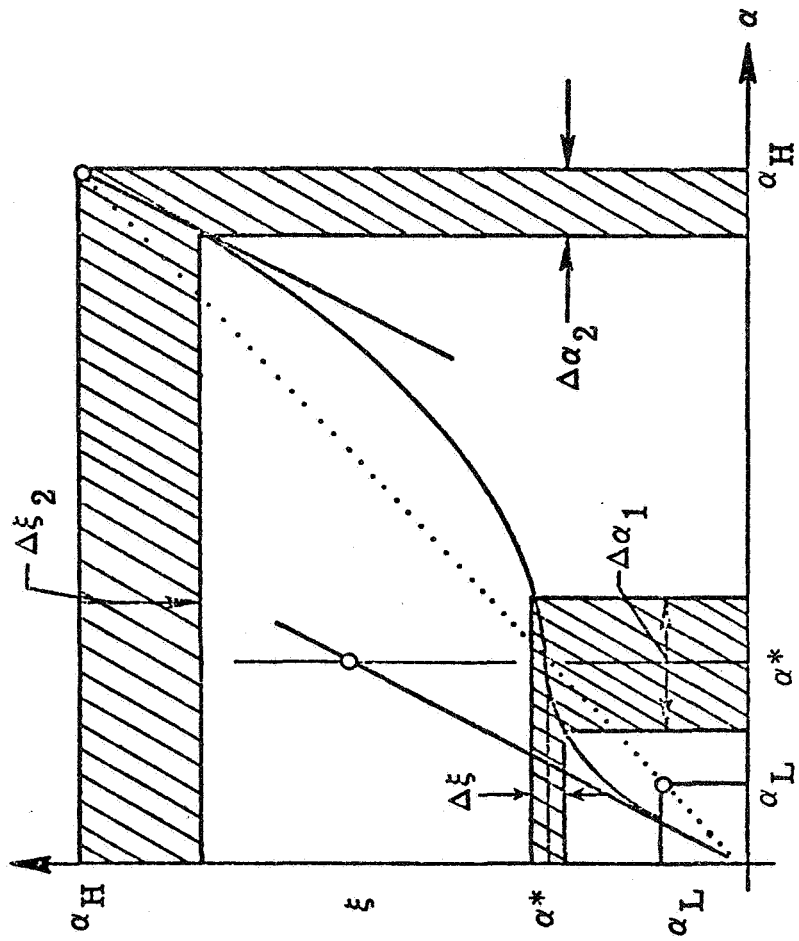


Figure A6.- Warping transformation.

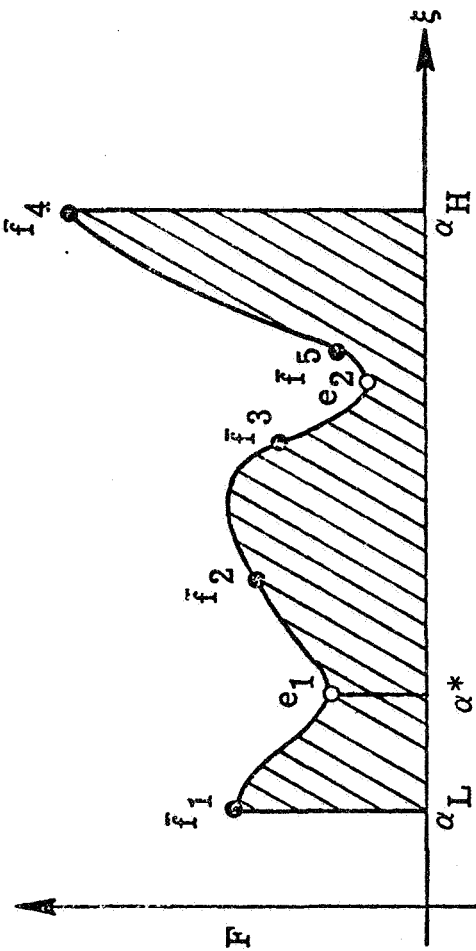


Figure A7.- Transformed function with two externals.

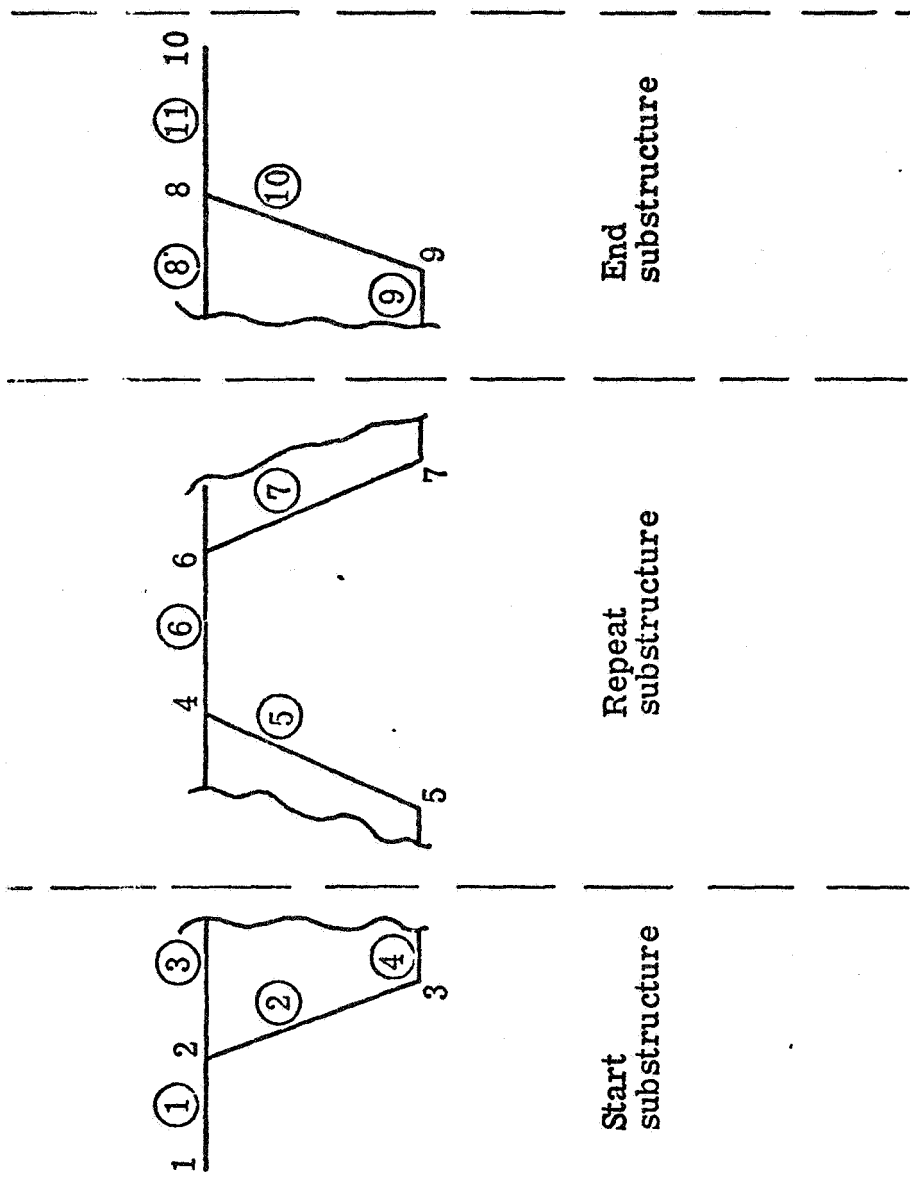


Figure B1.- Mathematical model for BUCLASP2.

TABLE - 1

<u>Graphite Epoxy</u>	<u>Aluminum</u>
$E_1 = 2 \cdot 10^7$ psi	$E = 10^7$ psi
$E_2 = 1.3 \cdot 10^6$ psi	$\nu = .300$
$G_{12} = 6.5 \cdot 10^5$ psi	$\rho = .100$ lbs/cubic inches
$\nu_{12} = .304$	or lbs/in <sup>3</sup>
$\rho = .055$ lbs/cubic inches	
or lbs/in <sup>3</sup>	

Material Properties

TABLE - 2

$f_1 = f_3 = f_4 = 0, f_2 = 100, L = 30$  inches

$\frac{Nx}{L}$	$\frac{W \cdot 10^4}{b L^2}$	$b_1$	$b_2$	$b_3$	$b_4$	$t_1$	$t_2$	$t_3$	$t_4$
1000	5.100	1.240	1.486	.605	.673	.134	.023	.500	.012
800	4.350	.964	1.510	.600	.600	.111	.025	.306	.016
500	3.300	.887	1.345	.300	.554	.081	.019	.444	.020
400	2.940	.782	1.280	.300	.475	.069	.018	.346	.014
300	2.490	.778	1.320	.300	.447	.066	.020	.196	.010
200	2.040	.610	1.200	.364	.367	.047	.017	.113	.010
100	1.460	.536	1.070	.308	.343	.035	.013	.067	.010
50	1.070	.530	.870	.300	.360	.028	.010	.051	.010

Optimized design variables for Graphite/Epoxy panel (L = 30 inches)

TABLE - 3

$f_1 = f_3 = f_4 = 0, f_2 = 100, L = 40$  inches

$\frac{N \times L}{L}$	$\frac{W \cdot 10^4}{b L^2}$	$b_1$	$b_2$	$b_3$	$b_4$	$t_1$	$t_2$	$t_3$	$t_4$
1000	5.200	1.350	1.970	.826	.490	.153	.030	.500	.027
800	4.600	.650	1.990	.460	.630	.060	.030	.500	.130
500	3.300	.845	1.830	.380	.600	.097	.028	.500	.015
400	3.010	1.100	1.680	.390	.668	.100	.023	.500	.013
300	2.480	1.020	1.650	.300	.560	.085	.023	.430	.010
200	2.020	1.070	1.860	.300	.630	.081	.023	.494	.014
100	1.450	.665	1.360	.400	.430	.044	.016	.102	.013
50	1.050	.380	1.200	.350	.350	.022	.013	.050	.018

Optimized design variables for Graphite/Epoxy panel (L = 40 inches)

TABLE - 4

$f_1 = f_3 = f_4 = 0, f_2 = 100, L = 50$  inches

$\frac{N \cdot x}{L}$	$\frac{W \cdot 10^4}{b L^2}$	$b_1$	$b_2$	$b_3$	$b_4$	$t_1$	$t_2$	$t_3$	$t_4$
1000	5.200	1.340	2.520	1.220	.650	.216	.040	.426	.010
800	4.500	1.500	2.560	.760	.730	.197	.040	.500	.027
500	3.300	1.330	2.500	.500	1.010	.176	.038	.500	.010
400	3.020	1.330	.219	1.250	1.080	.113	.033	.220	.070
300	2.500	1.170	1.900	1.000	.650	.080	.025	.140	.010
200	2.020	1.070	1.860	.300	.630	.081	.023	.490	.014
100	1.450	.930	1.580	.300	.570	.058	.017	.290	.014
50	1.030	.750	1.510	.300	.460	.042	.016	.105	.010

Optimized design variables for Graphite/Epoxy panel (L = 50 inches)

TABLE - 5

$f_1 = f_2 = 100, f_3 = f_4 = 0, L = 30$  inches

$\frac{N \cdot x}{L}$	$\frac{W \cdot 10^4}{b L^2}$	$b_1$	$b_2$	$b_3$	$b_4$	$t_1$	$t_2$	$t_3$	$t_4$
500	3.350	1.070	1.680	.550	.920	.021	.028	.500	.068
400	2.950	1.700	1.620	1.520	1.000	.033	.030	.171	.064
300	2.400	1.630	1.630	.640	.850	0.000	.032	.216	.060
200	2.080	.925	1.290	.830	.940	.015	.020	.136	.060
100	1.410	.865	1.160	.300	.674	.014	.016	.185	.036
50	.990	.787	1.010	.650	.520	.010	.013	.050	.023

Optimized design variables for Graphite/Epoxy panel (L = 30 inches)

TABLE - 6

$f_1 = f_2 = 100, f_3 = f_4 = 0, L = 40$  inches

$\frac{N_x}{L}$	$\frac{W \cdot 10^4}{b L^2}$	$b_1$	$b_2$	$b_3$	$b_4$	$t_1$	$t_2$	$t_3$	$t_4$
500	3.350	2.310	2.180	1.360	1.550	.048	.038	.470	.101
400	3.020	1.620	2.170	1.170	1.180	.031	.037	.351	.081
300	2.450	1.970	2.080	1.600	1.170	.038	.038	.172	.075
200	2.020	1.170	1.850	.800	.980	.021	.030	.200	.064
100	1.430	1.500	1.610	1.210	.820	.026	.023	.094	.035
50	.995	1.010	1.330	.590	.720	.013	.016	.098	.032

Optimized design variables for Graphite/Epoxy panel (L = 40 inches)

TABLE - 7

$f_1 = f_2 = 100, f_3 = f_4 = 0, L = 50$  inches

$\frac{N \cdot x}{L}$	$\frac{W \cdot 10^4}{b L^2}$	$b_1$	$b_2$	$b_3$	$b_4$	$t_1$	$t_2$	$t_3$	$t_4$
500	3.320	2.400	2.650	1.500	1.540	.030	.040	.240	.080
400	2.990	1.990	2.760	1.150	1.390	.051	.049	.500	.084
300	2.520	2.810	2.800	1.850	1.170	.065	.052	1.253	.048
200	2.020	1.220	2.150	1.870	1.360	.021	.033	.180	.085
100	1.450	1.620	1.840	1.520	1.160	.030	.023	.142	.046
50	1.000	1.820	1.680	.970	.920	.023	.021	.123	.034

Optimized design variables for Graphite/Epoxy panel (L = 50 inches)

TABLE - 8

All Aluminum section, L = 30 inches

$\frac{N \times}{L}$	$\frac{W \cdot 10^4}{b L^2}$	$b_1$	$b_2$	$b_3$	$b_4$	$t_1$	$t_2$	$t_3$	$t_4$
500	8.330	3.420	1.613	2.960	1.880	.139	.058	.199	.010
400	6.720	2.850	1.670	2.670	1.545	.112	.063	.113	.010
300	5.560	2.418	1.650	2.175	1.340	.091	.059	.082	.010
200	4.450	1.800	1.474	.300	1.040	.062	.048	.399	.010
100	3.150	1.710	1.270	1.540	1.020	.049	.035	.046	.010
50	2.210	1.205	1.097	1.160	.810	.029	.026	.029	.010

Optimized design variables for all aluminum panel (L = 30 inches)